IN-75
71278

NASA Technical Memorandum

NASA TM-86583

AN EXPERIMENTAL STUDY OF LASER-SUPPORTED PLASMAS FOR LASER PROPULSION - FINAL REPORT

Center Director's Discretionary Fund Project DFP-82-33

By R. H. Eskridge, T. D. McCay, and
D. M. Van Zandt

Propulsion Laboratory
Science and Engineering Directorate

January 1987

National Aeronautics and
Space Administration

George C. Marshall Space Flight Center

MSFC - Form 3190 (Rev. May 1983)

TABLE OF CONTENTS

LIST OF ILLUSTRATIONS

LIST OF SYMBOLS

g	acceleration due to gravity
γ	ratio of specific heats of the working fluid
$\bar{R}$	universal gas constant
Tc	chamber temperature (K)
M	molecular weight of working fluid
Pe	nozzle exit pressure (Pa)
Pc	chamber pressure (Pa)
Isp	specific impulse (sec^{-1})
C1	constant in the free-bound radiation formula
C2	constant in the free-free radiation formula
E	energy of the nth level (ergs)
ε_o	permittivity of free space [8.854E-12°C (N-m)]
ε_ν^{ff}, ε_ν^{fb} ε_ν^{ℓ}	emission coefficients of free-free, free-bound, and line radiation, respectively
g_k	statistical weight of the kth level
$G^{ff}(\nu)$	Gaunt factor for free-free radiation at frequency, ν
$G_n^{fb}(\nu)$	Gaunt factor for free-bound radiation at level n, and frequency, ν
h	Planck's constant (6.626E-27 erg-sec)
I(x)	radiance of the plasma [$W/(cm^2$ sr Hz)]
k	Boltzmann's constant (1.38E-16 erg/K)
m0	mass of the electron (9.107E-28 gm)
Ne	number density of electrons (cm^{-3})
N_z, N_{z-1}	number density of successive ionization stages
P	pressure of the plasma ($dynes/cm^2$)
r	radial coordinate (cm)
T	plasma temperature (in the equilibrium sense) (K)

LIST OF SYMBOLS (Concluded)

Te	electron temperature
U_z, U_{z-1}	partition functions for successive ionization stages
ν	frequency of plasma radiation (Hz)
x	spatial coordinate (cm)
χ_{z-1}	ionization potential of the atom (ergs)
$\Delta\chi_{z-1}$	lowering of the ionization potential due to the presence of other atoms
z	number of electronic charges that the radiating electron "senses," z-1 is therefore the charge of the ion

TECHNICAL MEMORANDUM

AN EXPERIMENTAL STUDY OF LASER-SUPPORTED PLASMAS FOR LASER PROPULSION - FINAL REPORT

Center Director's Discretionary Fund Project DFP-82-33

INTRODUCTION

The civilian space flight missions being contemplated in the 1990's center around large structures operating at altitudes significantly above those serviced by the space transportation system, i.e., the space shuttle. The fact that such large structures will represent very large masses which must be moved to high orbits begins to stretch the imagination of the propulsion engineer. Contemporary propulsion systems suffer significantly when asked to raise such large masses. Capable of large thrusts, they operate at relatively low efficiencies and, thus, their payload mass fractions are quite low. For many applications, this almost precludes their usefulness. Furthermore, reliable high efficiency systems are not currently available except for very low thrust devices. In many respects, low thrust level can be an attribute, especially when moving large flexible structures. Too small a thrust (subpound), however, leads to abnormally long (several years) trip times to move massive structures to high orbits. Thus, the need for at least moderate thrust, but high performance propulsion systems, is established. NASA/Marshall Space Flight Center (MSFC) is investigating a potential fulfillment to that need, the hydrogen-fueled laser thermal rocket. This concept uses a hydrogen plasma as the "combustion" source which can theoretically be sustained and controlled to provide significant thrusts (hundreds of pounds) and high specific impulse (2500 sec) using currently envisioned laser systems. Figure 1 indicates how such a system fills the need under discussion.

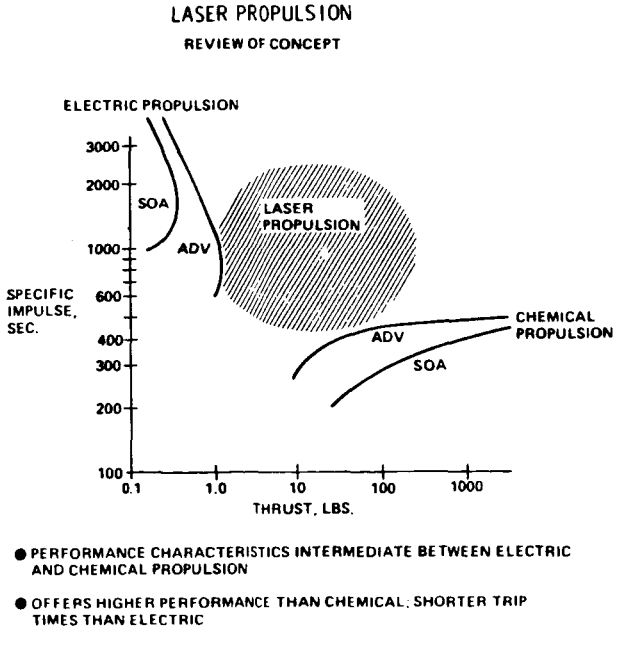

Figure 1. Performance and thrust for rocket engine systems.

Basic research has been conducted to elucidate the physics associated with laser sustained hydrogen plasmas. Inverse Bremsstrahlung absorption by the free electrons within the plasma is the energy conversion mechanism upon which the laser thermal thruster concept is predicated. The effort discussed herein is a report on the progress of that research. An introduction to some of the aspects of that research effort includes a discussion of the characteristics of such a thruster, realistic performance levels, the pulsed laser spark ignition scheme now developed, and the diagnostics developed to completely characterize the properties of the laser sustained hydrogen plasmas.

LASER THERMAL THRUSTER

The laser thermal thruster, in concept, is a relatively simple device as schematically presented in Figure 2. The hydrogen plasma can be considered analogous to the flame combustion region which exists in a conventional rocket engine. The conventional system uses the internal chemical energy of the propellants as its source of enthalpy whereas the laser thruster depends upon an external source, the electromagnetic energy contained within the sustaining laser beam. The hydrogen plasma performs the work of both reactant and product, i.e., the electrons within the plasma absorb the laser energy and the high enthalpy plasma is the high temperature region which expands for thrust production. Thus, once the energy is absorbed the thruster behaves in a conventional manner. In practice, the propellant would probably be distributed through the thruster walls as a regenerative coolant, then injected into the absorption chamber, heated by the plasma, and expanded out a nozzle for thrust generation.

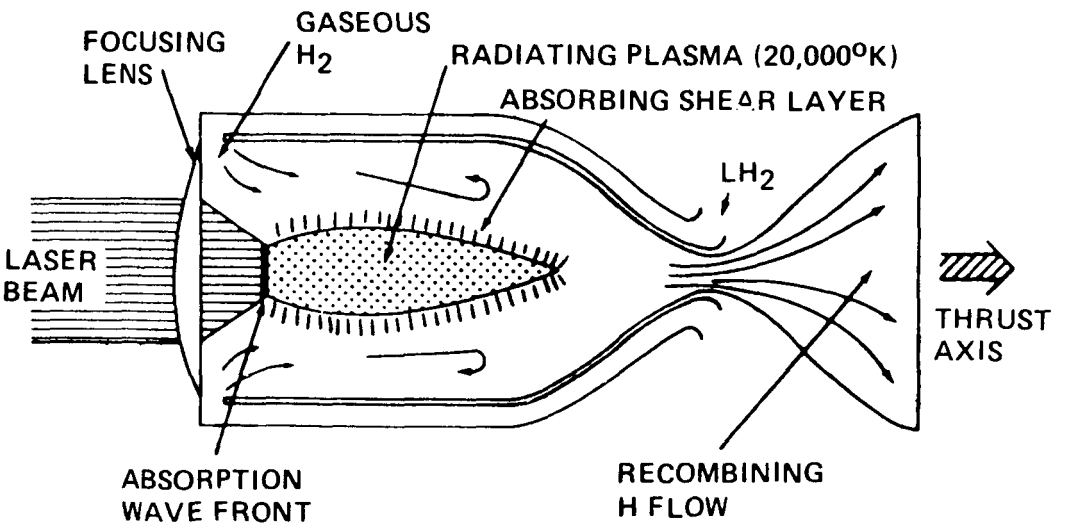

Figure 2. Schematic of a hydrogen-fueled laser thruster.

Although a large variety of absorbing gases could be used for such a concept, hydrogen is the optimum choice as a working fluid because of its high performance, i.e., specific impulse and also good radiative transfer characteristics. The work of Shoji [1] showed this to be the case, as born out by simple inspection of the equation for specific impulse, which shows the simple dependence:

$$Isp = \sqrt{\frac{1}{g}\frac{2\gamma}{\gamma-1}\frac{\bar{R}\,T_c}{M}\left[1-\left(\frac{Pe}{Pc}\right)^{\gamma-1/\gamma}\right]} \qquad (1)$$

In the case of a hydrogen plasma, an obvious minimum in molecular weight is obtained and that, coupled with practical gas bulk temperatures of over 3000K, makes it the most attractive of all gases from a pure performance point of view. When one includes the effect of storage (tankage), that edge is diminished somewhat but hydrogen remains the leading candidate. This research has, therefore, concentrated exclusively on investigating the physics of laser-sustained hydrogen plasmas. The following section addresses a practical aspect of the utility of a hydrogen plasma once it is created, how effectively can the available energy be extracted.

CHEMICAL KINETIC LIMITATIONS

Even if all goes perfectly with regard to beaming and converting energy, there are still realistic concerns with regard to the performance of such a thruster. This is both in the sense of pure theoretical specific impulse and with regard to the many practical concerns such as whether the laser windows and thrust chamber will even survive. These survival problems are real but can probably be engineered if the payoff potential is sufficient. Chemical kinetic and pure fluid mechnical limitations are, on the other hand, not as easily engineered. The fundamental physics cannot be avoided and one must pay for the losses inherent in the physics. If these losses can be established as manageable or tolerable then further investigation into the overall concept is warranted. In such a vein, the kinetic losses (only) for a typical laser thermal thruster were examined. Recognizing that a large fraction of the potentially useful enthalpy is tied up in the dissociation and ionization energies, it is mandatory that sufficient recombination energy be extracted to keep specific impulse at a viable level.

A parametric study of the specific impulse obtainable for a prototype thruster was performed. The parameters examined included the chemical kinetic rates, combustion chamber pressure, combustion chamber (bulk gas) temperature, and nozzle area ratio and half angle. The chemical kinetic rates were chosen based upon the best available literature for the hydrogen reaction system. The kinetic rates were chosen as a baseline and a worst case set of rates were determined by reducing the rate of coefficients by a factor of 10. This permitted an evaluation of the maximum reduction of specific impulse which might occur even if the rates were uncertain by more than the experimental estimates. The evaluation was performed in a manner very similar to that taken by Bray [2] in his study of recombination energy losses within supersonic nozzles. A one-dimensional inviscid analysis has currently been performed but an interest in eventually examining two-dimensional nonuniform flow and viscous layer effects dictated the choice of a versatile computational tool with such capabilities. The Two-Dimensional Kinetics (TDK) computer code [3] was thus chosen since it has those attributes. As mentioned, however, for the work reported here only the one-dimensional kinetics (ODK) option was used. In addition to the kinetics calculations, the computations were also performed for both equilibrium and frozen chemistry assumptions to permit more complete comparisons to be made. Complete details of the chemical kinetic calculations performed have been published elsewhere [4].

A total of 432 cases were run using the ODK code. Typical results are shown in Figure 3 which depicts the predicted specific impulse as a function of initial chamber temperature. For temperature levels believed to be compatible with heat transfer considerations (below 5000K), large differences in the performance is realized for the three sets of rates. The difference between equilibrium and frozen is over 500 sec at 6000K, for example.

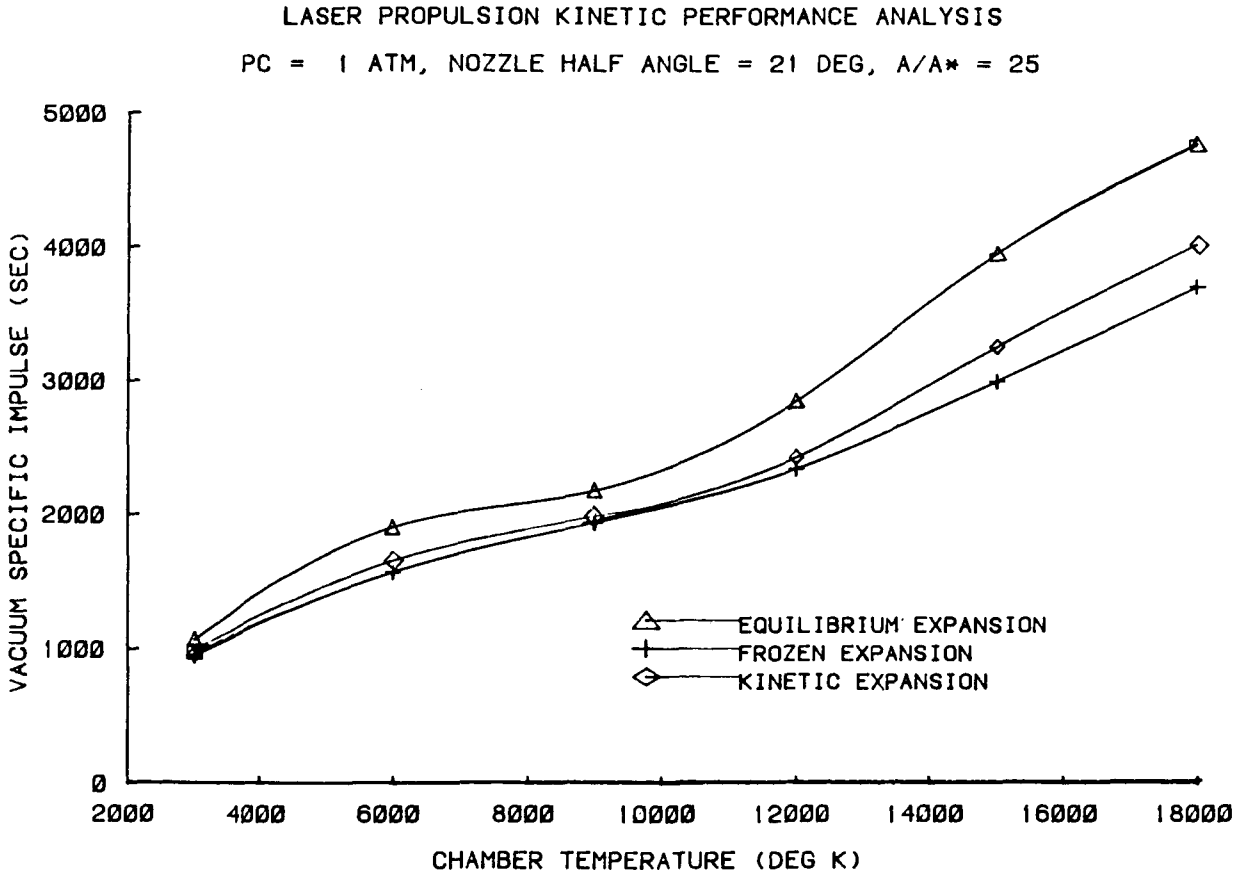

Figure 3. Laser propulsion kinetic performance analysis.

The curves in Figure 3 can be used to make several points. First, improvement in specific impulse does not increase significantly between 6000 and 9000K. Since radiation losses are not included in the ODK analysis, it appears that attempting to operate a thruster above 6000K would not be very fruitful from a performance point of view. Also, for the simple convergent/divergent nozzle considered here, a considerable performance loss due to nonequilibrium chemistry is realized. The best kinetics data shows over a 100 sec Isp loss for a chamber temperature of 5000K. Another interesting effect not shown by Figure 3, but which was a product of the ODK study, is the effect of nozzle expansion ratio. It is quite interesting that further performance gain from nozzle expansion is not realized for area ratios greater than 5. Thus, very small "nozzleless" thrusters can be contemplated for the thrust class considered here (100 lbf). This is, of course, attributable to the low chamber pressures and the quick freezing of hydrogen atoms just downstream of the nozzle throat.

The purpose of this discussion is not only to indicate that kinetics is important but that this class of propulsion device with very high specific impulse can be drastically affected by normally small effects. Future work will evoke two-dimensionality and viscous effects to evaluate additional performance losses which must be anticipated.

Regardless, just the kinetic study shows that a 1500 sec Isp is a more realistic estimate than the 2500 sec generally quoted in the literature.

EXPERIMENTAL EFFORT

The experimental program now being conducted [5] has been broken down into two distinct efforts, hydrogen plasma ignition experiments and steady-state hydrogen plasma experiments. The ignition experiments have been completed and are discussed in some detail in the following sections. The steady-state hydrogen experiments are still continuing, but a description of the progress to date is included.

Hydrogen Plasma Ignition

The power available from conventional cw lasers is not sufficient to initiate a laser supported plasma due to the high breakdown threshold and low absorptivity of cool gases. To create and then sustain a laser-supported plasma, an adequate source of free electrons must be made available to absorb the incident laser energy. This source of electrons can be obtained by a variety of methods. Smith and Fowler ignited laser-sustained plasma by using both electrical discharges [6] and by laser impact onto solid targets [7]. Moody [8] ignited laser sustained plasmas using the gas breakdown produced by a pulsed CO_2 laser.

A pulsed CO_2 laser has been chosen to achieve plasma ignition. This method was selected as being the cleanest, least intrusive and most reliable of the available options that have been previously demonstrated. To achieve reliable ignition using this technique, it is necessary to superimpose the focal volume of the pulsed laser onto the focal volume of the sustaining (steady-state) laser beam. Since these focal volumes must be very small to produce the required large energy densities, alignment is critical.

In the past, pulsed CO_2 laser ignition has been used in two different ways. Moody [8] injected the pulsed CO_2 laser beam as close to on-axis as possible to the main beam and Fowler et al. [9] injected the pulsed beam normal to the main beam. The approach taken in this study is unique in the fact that advantage is taken of the unstable resonator output of the MSFC high energy cw laser. The output profile of the cw laser resembles a torus with near zero power at the center of the beam. The pulsed CO_2 laser beam is injected coaxial with the main beam through a hole in the main beam turning mirror. The advantage of using this technique is the ease of alignment of the two focal volumes and minimum required optical components.

The pulsed laser produces a spark within the gas, a high electron density region which can precipitate a sustained plasma. The characteristics of the pulsed CO_2 laser spark were initially examined to determine the spatial location of the maximum electron density, the gas breakdown threshold, and the fraction of pulsed beam energy absorbed as a function of hydrogen pressure. This was done in an attempt to provide sufficient characterization of the spark to use it to ignite the cw laser sustained plasmas.

The experimental setup for the laser spark experiments is shown schematically in Figure 4. The laser used was commercial Lumonics 103 TEA laser equipped with 0.09 microfarad capacitors. The energy and pulse length delivered were 7 Joules

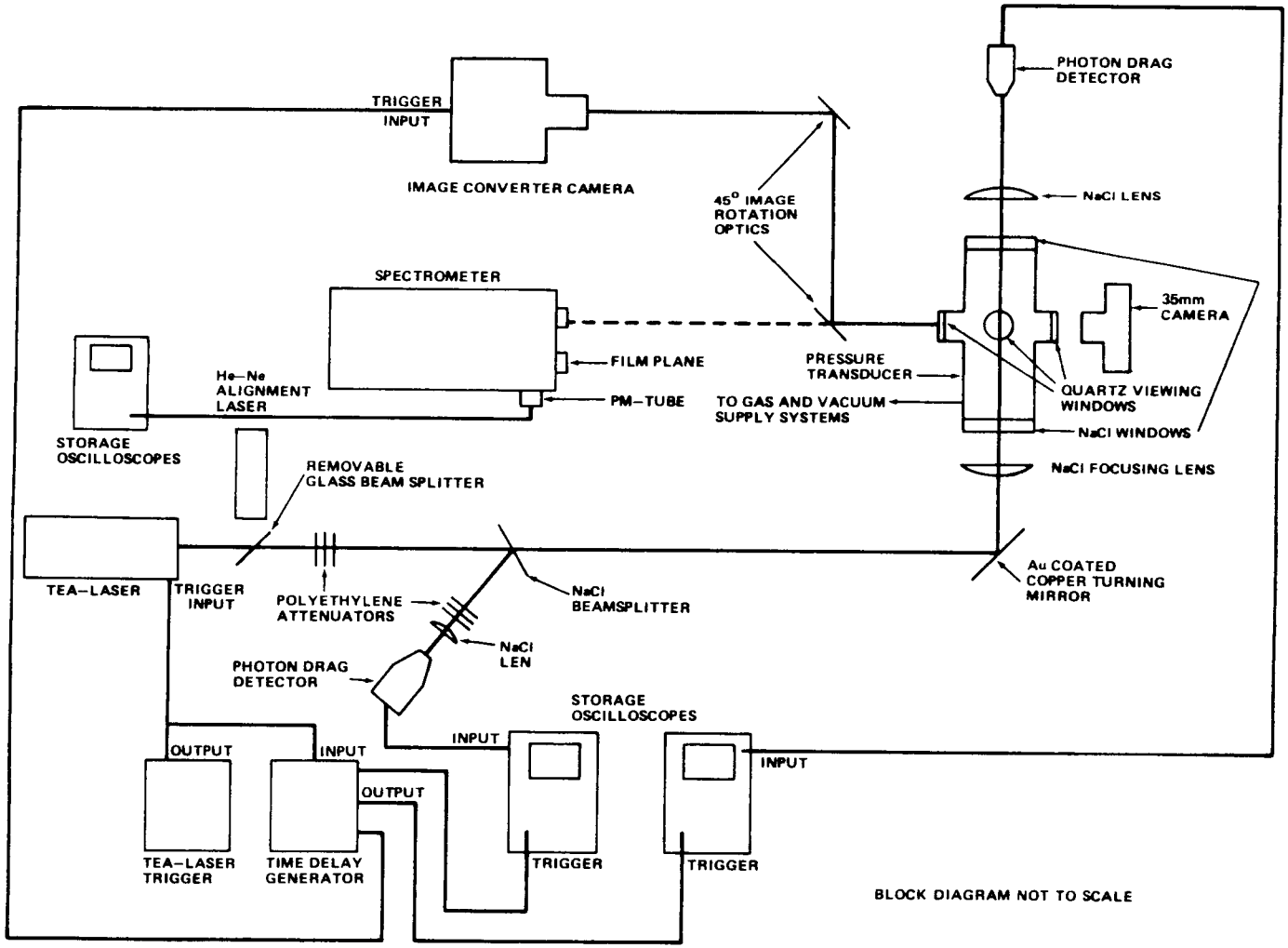

Figure 4. Pulsed laser spark experiments schematic.

at 150 nanosec per pulse through unstable resonator optics. The output beam was directed through a variable number of polyethylene attenuators and turned up into the hydrogen test cell.

The hydrogen test cell is a cylindrical, 15 cm diameter, 40 cm long, black anodized aluminum chamber. The hydrogen pressure within the cell can be remotely controlled from less than 0.1 atmospheres up to approximately 5 atmospheres, the limit being based upon the yield strength of the NaCl windows. All the spark data were taken statically with regard to cell gas flow and no perceptible global temperature rise within the cell was observed for any test situation.

The diagnostics employed consisted of systems for the measurement of incident and transmitted beam power and for optical observation of the spark itself. An STL Image Converter Camera was used to record streak photographs of the spark behavior. Typically, the streak times were approximately 200 nsec in duration. A two-mirror viewing system permitted the upbeam propagation of the breakdown plasma luminous front to be recorded. In addition to the streak photographs, frame photographs were obtained at various exposure levels and interframe delay times using an STL Model 4A (3 frame) Frame Unit. The remaining diagnostics consisted of simple 35 mm open shutter closeup photography and spectrographic surveys. A 1.25 m Spex Model 1269 f/9 scanning spectrometer with both photographic plate and photomultiplier outputs was employed to examine emission from the spark. A pair of flat UV overcoated mirrors allowed the spectrometer entrance slit to be focused at several locations within the plasma to examine the spatial dependence of radiance. Photographic plates and photomultiplier data were taken to permit integrated intensity and temporal radiance behavior to be examined, thus indicating the spatial location of maximum electron density.

Steady-State Hydrogen Plasma

The steady-state hydrogen plasma is the key element of the laser propulsion concept. Although there is a significant amount of data on laser sustained plasmas in several gases, there is very little data available for hydrogen. The major thrust of this program is to obtain and evaluate plasma influencing parameters and determine the feasibility of the laser supported hydrogen plasma as a candidate for enthalpy source for further thruster development. These parameters are the fractional absorption of beam power by the plasma, i.e., the conversion of plasma energy to propellant enthalpy, the chamber wall heat loading, and the fluid dynamic stability of the laser sustained plasma.

Steady-state laser plasmas have been reported by several investigators, including Conrad [10], Keefer [11], and Smith [6,9]. These plasma experiments have been conducted in atmospheric air and inert gases, particularly argon. They concluded that a laser plasma can be maintained in a steady-state for indefinite periods of time and can be created in any gas, if the proper irradiance, pressure, and temperature criteria can be met.

A laser-supported plasma is created when the irradiance at the focus of the laser beam exceeds the ignition (breakdown) threshold irradiance of the gas at a given temperature and pressure. Once these conditions have been achieved, only a maintenance threshold irradiance need be supplied to sustain the plasma. This threshold for maintenance of the plasma is typically orders of magnitude lower than the threshold for plasma ignition.

Laser-supported plasmas normally propagate from the focus of a high-energy laser beam back toward the laser. During this propagation upbeam, the plasma may extinguish if the beam spread is such that the maintenance energy threshold is not maintained along the beam. In this case, the laser plasma either completely disappears or, if the required ignition conditions are present, reforms back at the focus. If it reforms then the cycle repeats itself. Once the plasma is created, it can be convectively stabilized, either by free convection if small f-number optics are used, e.g., f/8 or lower, or by forced gas counterflow for larger f numbers. For a vertically oriented plasma, the natural convection through the plasma (due to buoyancy effects) can be sufficient to provide the stabilizing counter flow. This free convective stability point is near the maintenance threshold irradiance and does not produce as high a plasma temperature as possible if it were a region of higher irradiance. The plasma may be forced farther downbeam by the application of a forced external flow. This method offers the ability to force-convectively stabilize the plasma and control the position with respect to irradiance level within the laser beam. Conrad demonstrated that the position of the plasma, with respect to the irradiance level, does control the laser beam absorption and thereby the plasma temperature. In order to operate a laser thruster in an efficient manner, laser beam absorption must approach 100 percent. Based upon Conrad's work in air at 1 atmosphere, it appears that this goal is obtainable.

The experimental objectives are to determine the minimum irradiance threshold of a hydrogen plasma, the spatial temperature distribution whtin the plasma, and energy emission of the plasma as a function of pressure, beam power, and imposed flow conditions. This will then provide a sufficient data base to design and evaluate laser thrusters operating with laser sustained hydrogen plasmas.

The lasers used in this exxperiment are a 30 kW closed-cycle cw CO_2 electric discharge laser and the Lumonics 103 CO_2 TEA laser. The output beam of the 30 kW laser is collimated and directed via gold-coated copper mirrors and focused into the plasma chamber. The plasma chamber is a 15 cm diameter, 40 cm long water-cooled cylinder. The chamber has been black-anodized to reduce stray reflections and also to serve as an absorber for wall thermal loading measurements. Figure 5 gives a schematic of the plasma chamber and the associated beam delivery optics.

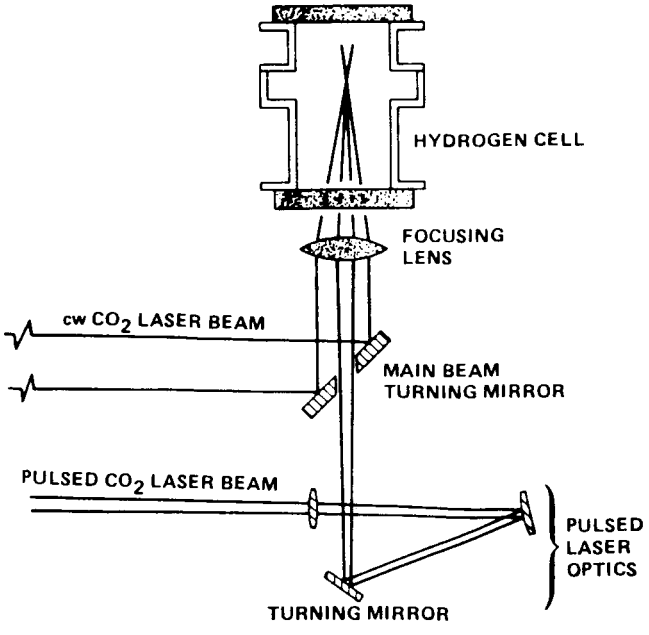

Figure 5. Test chamber schematic - laser plasma experiments.

A plasma is initiated in the test chamber by a single TEA laser pulse focused coincident with the main 30 kW cw beam. Once the plasma has been ignited, a variety of diagnostics are employed for data acquisition.

The plasma energy coupling is measured by determining the main beam transmission through the plasma. The main beam power is initially measured with a Coherent Model 213 power meter before entering the test cell, and by a 25 cm water-cooled ball calorimeter after leaving the test cell. The difference between these two measurements yields the transmitted power. These measurements are taken for a variety of power levels, pressures, and plasma locations with respect to the focus.

The plasma location is varied by using a gas flow in opposition to the natural plasma propagation upbeam. This flow is throttled to obtain the specified flowrates and chamber pressures of interest. The flow is ultimately exhausted through a vacuum pump to a vent stack for disposal. The thermal wall loading produced by the plasma is estimated in three ways. First the test chamber is water-cooled to permit bulk calorimetric measurements of the chamber wall thermal loading. In addition, two optical estimates of the radiative losses are made using a scanning radiometer and an optical spectrum analyzer.

The plasma temperature is determined by a diagnostic technique based on an absolute measurement of plasma continuum radiation. The data is taken using a calibrated video camera and a narrow band-pass filter. The radial distribution of plasma emission coefficient is determined for each video scan line through Abel inversion. A temperature value is assigned to each radial location by correlation with theoretical emission calculations obtained using the assumption of local thermodynamic equilibrium. The result is the three-dimensional spatial distribution of temperature within the plasma. This temperature field is useful for integration of plasma conduction and radiation losses. The absorption of the incident laser power may then also be tracked through the plasma using the temperature data and the relation for inverse Bremsstrahlung radiation. A description of the diagnostics employed for these measurements is available in the appendix.

EXPERIMENTAL RESULTS

Plasma Ignition Experiments

The first experimental parameter examined was the breakdown threshold of hydrogen. Since the control of breakdown is key to future later thruster development work and since hydrogen breakdown intensity measurements do not abound in the literature, it was the central measurement in the ignition phase of the study. The determination of breakdown intensity naturally requires a knowledge of the focal area. Since the beam intensity pattern did not lend itself to a facile estimate of the focal area, it was experimentally determined by axially varying the location of thermal sensitive paper throughout the focal region. Using this approach, the focal diameter of the laser beam was determined to be 0.01 cm. That diameter was employed for all subsequent intensity calculations. Based on estimates of the thermal paper sensitivity, this diameter corresponded to a diameter slightly larger than the 1/e point.

The breakdown or threshold intensity, as it is sometimes called, is somewhat of a nebulous term. To begin with, the definition of this intensity is that which provides gas breakdown at least one half of the time. Breakdown is generally accepted to be determined by observing a flash in a darkened room. Assuming it to be an

off/on phenomenon, this is a reasonable, although qualitative, criteria. Since the spark is associated with a pulsed system, there are other ambiguities which enter into the analysis of the breakdown intensity. For most cases reported in the literature, the breakdown intensity is given but there is no indication of whether that intensity is computed using a peak power during the pulse, average power in the pulse, or some other measure. For a mode spiking system, the difference in the various choices can be considerable. In addition to that concern, the distribution of energy at the focus is significant, as is the pulse length. Most researchers choose to assume a Gaussian intensity distribution at the focus, which is probably incorrect for most cases. The effects of pulsed duration have been shown to also be significant but no general approach to accounting for pulse length has been recommended. Based upon the assumption that most previously reported data for breakdown threshold is given in terms of average intensity within the pulse, the data in Figure 6 is presented in that format. These data demonstrate the pressure dependence of hydrogen breakdown intensity over the very limited pressure range of interest in these experiments. The recorded intensity levels compared favorably with those for particulate free air, helium, and other gases. These breakdown intensities are estimated to be accurate within 50 percent. It should be recalled that some dependence upon both pulse length and focal diameter has been previously noted [12]. This investigation did not study the variation of either of those parameters except for the small changes inherent in the shot-to-shot laser energy variance. The behavior of breakdown intensity at the lowest pressure (0.5 atmospheres) was quite unexpected and those data have been re-examined to assure that the cell evacuation procedure did not introduce impurities into the measurement breakdown intensity. The behavior at the higher pressures is consistent with the collision dominated cascade breakdown mechanism. These breakdown intensities will now serve as the baseline estimates for the necessary levels of pulsed power which must be available for routine ignition of a clean hydrogen plasma. Currently, the low values for the 0.5 atmosphere case appear to be correct, although still unexplained.

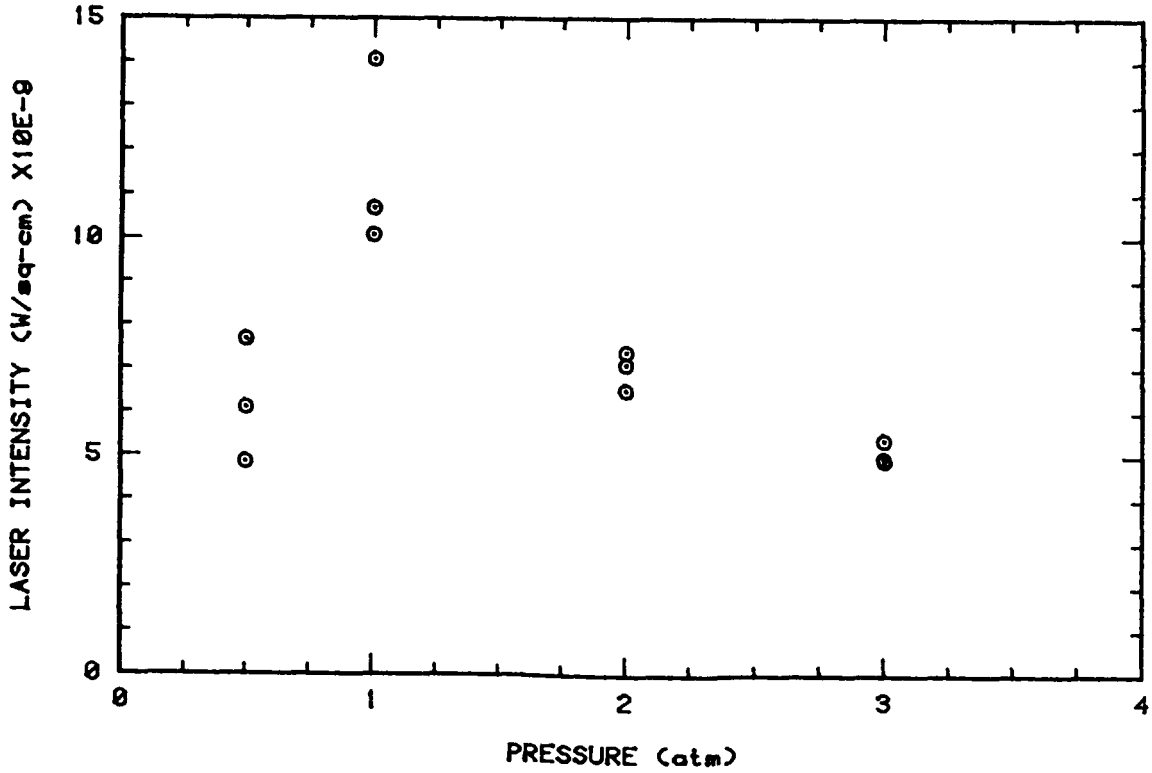

Figure 6. Measured breakdown intensity for pure hydrogen gas.

Figure 7 presents the results of the simultaneous measure of transmitted energy using a second photon drag detector. These data compare qualitatively with those reported for air by Caressa [13], although his data covered much higher energies. Caressa concluded that the f number was very critical with regard to the transmitted power. In this investigation, only the operational f number, approximately 12, was examined. Figure 7 does not indicate a strict transmission cutoff with regard to breakdown initiation. Although the functional dependence is quite steep, it does appear to be a smoothly varying function of input intensity (energy) and thur the mechanism which initiates breakdown appears to still be involved in the inception region. Included in these points are data both with and without observed breakdown flash. It is noteworthy that near an intensity of 7×10^9 W/cm^2, a significant break in the data occurs. This corresponds to the average breakdown intensity for the pressure range covered, not surprising but nevertheless interesting. Figure 7 does not seem to indicate any pressure dependence of the transmittance, although that dependence could easily be hidden in the considerable data scatter.

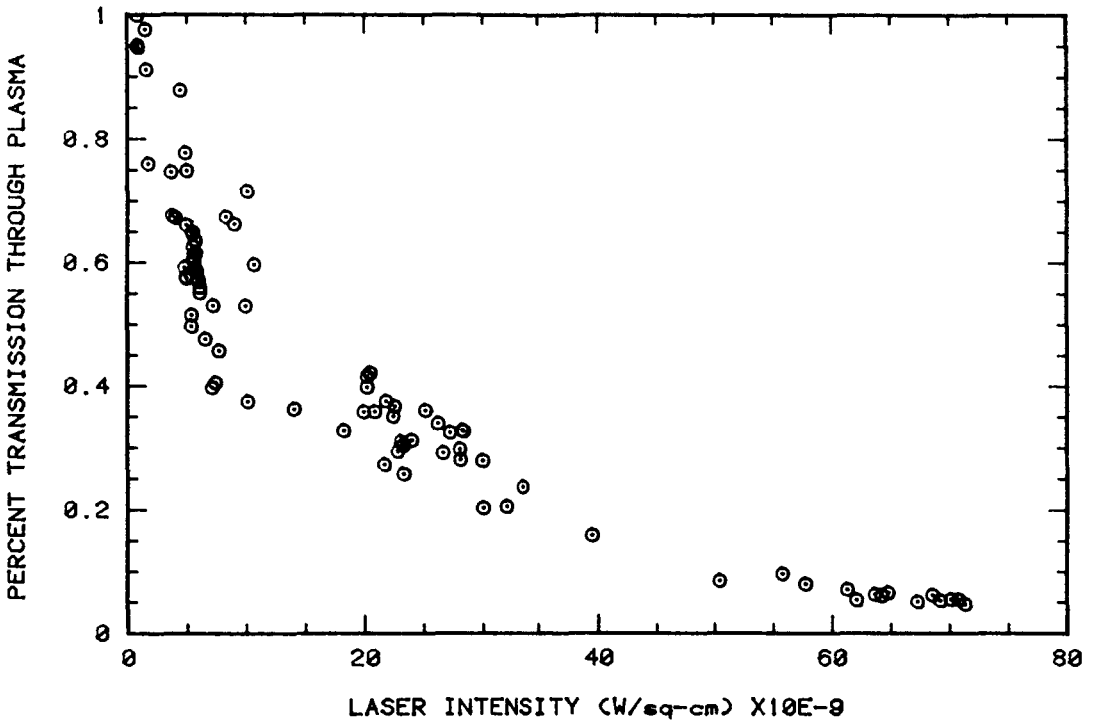

Figure 7. Laser transmission as a function of input intensity.

The final type of data taken was spectroscopic. The spectrograph was used to examine the Balmer series from alpha to delta. Figure 8 shows typical densitometer data for the indicated emission line at 3 atmospheres pressure. A data scan for 0.5 atmospheres has been added to show the effect of pressure on line broadening. There was not sufficient light to permit single shot spectra to be obtained and thus these densitometer data traces represent photographic plate density for 100 exposures. In the initial attempts to gather these spectra, the spectrometer slit was focused near the TEA laser focal point. Repeated attempts at obtaining spectra showed the gas to be too cool in that region, with only minimal radiation in terms of either line or continuum. The data in Figure 8 is for a spatial location about 2 cm upbeam. The slit height (2 mm) was sufficient to permit the intensity gradient to be examined at that general location. The three data scans in Figure 8 represent the upper, middle, and lower locations within the 2 mm. As can be seen from the increased broadening

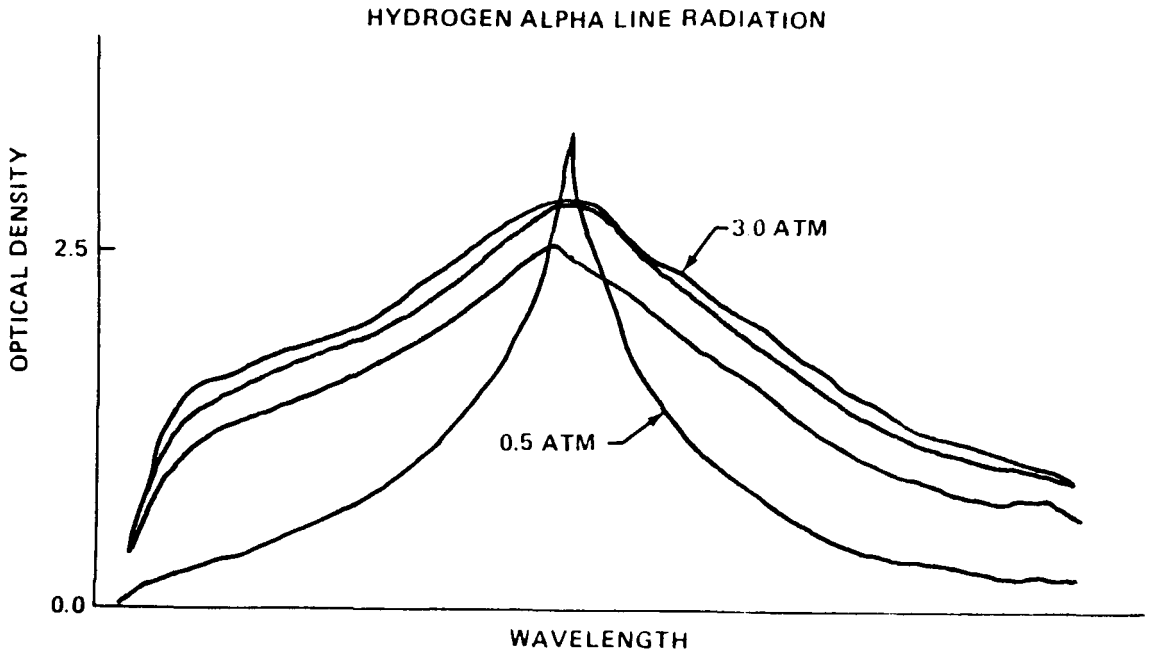

Figure 8. Hydrogen alpha line radiation at various pressures.

upbeam, the electron density within the spark plasma increased in that direction. The temperatures near the 2 cm point have been estimated to be approximately 18,000K based on the H line-to-continuum ratio.

It does appear that nonequilibrium processes are involved since the ratios for beta and shorter wavelengths indicate much higher pressures, but further data reduction would be necessary to provide publishable estimates. The 18,000K temperature is noted to correspond closely with the 17,400K absorption maximum which occurs for hydrogen inverse Bremsstrahlung.

Steady-State Plasma Experiments

The experimental study of the maintenance of a steady-state plasma in hydrogen has not yet been accomplished due to problems with the NASA-Marshall 30 kW cw laser. These problems have only recently been corrected by replacement of the main laser cavity blower motors. Some steady-state plasma results have been obtained for argon which was used during system checkout. These preliminary tests demonstrated the validity of the TEA laser coaxial ignition technique.

Radiance data was obtained for a two atmosphere argon plasma. A radiance profile plot for the plasma is shown in Figure 9. The reduction of this data from radiance to gas temperature has also been completed using Abel inversion and argon continuum emission data. Temperature profiles for the 2 atmosphere argon plasma are shown in Figure 10. It is interesting to note that the maximum temperature (16,500K) closely corresponds to the predicted maximum temperature of the argon plasma of 16,800K.

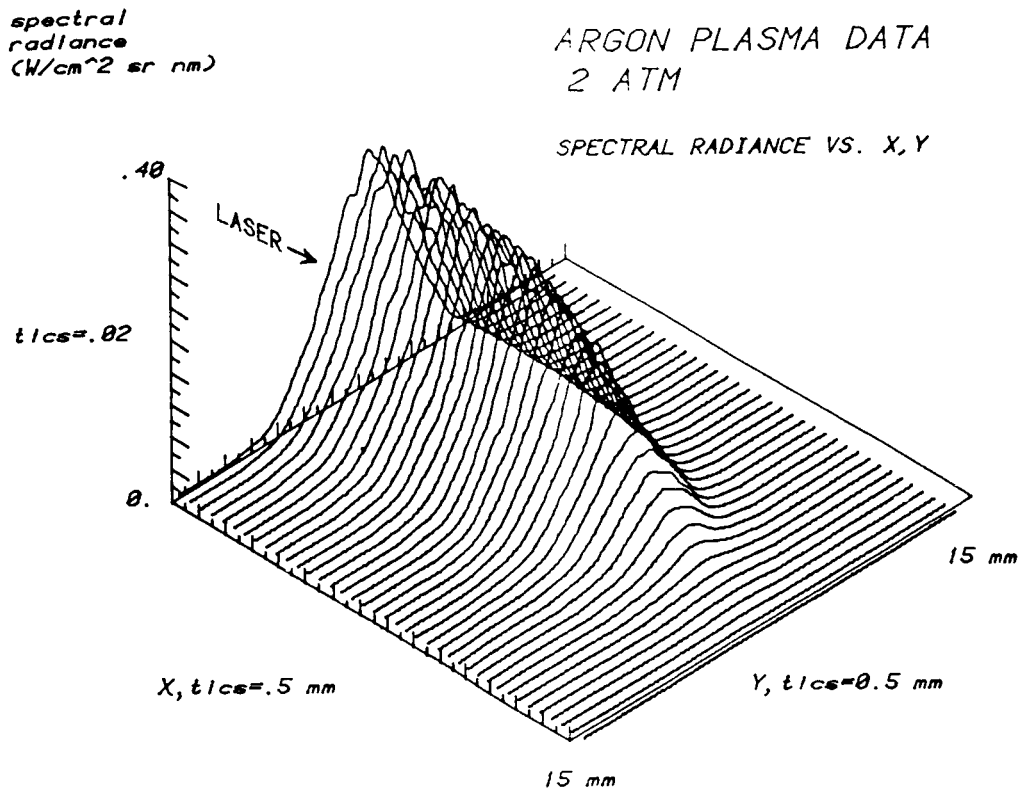

Figure 9. Radiance data for a 2 atmosphere laser plasma in argon.

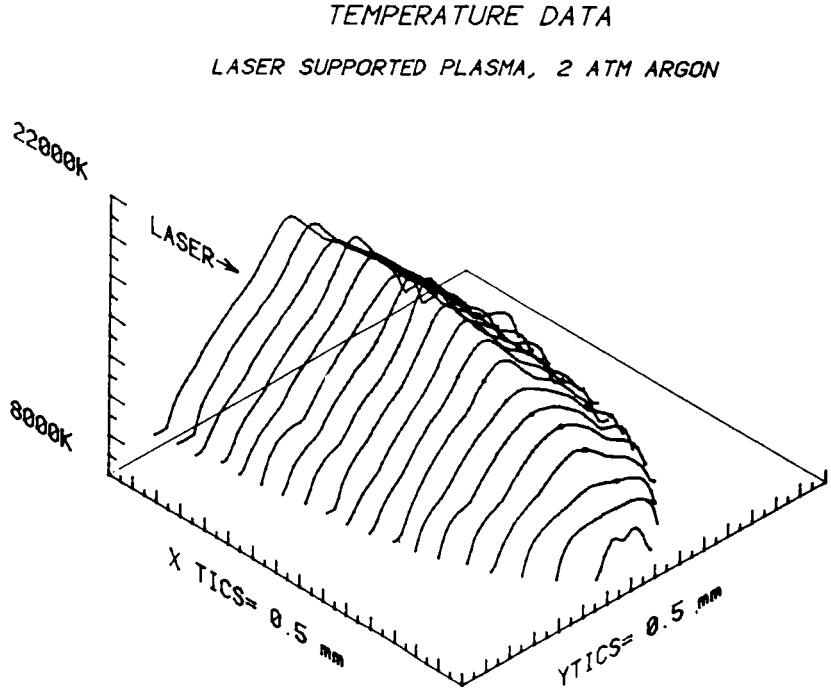

Figure 10. Calculated temperature profiles for a 2 atmosphere laser-sustained plasma in argon.

CONCLUSIONS AND FUTURE WORK

An experimental and theoretical study has been undertaken to determine the feasibility of a rocket thruster which receives its enthalpy from remotely beamed laser energy. A chemical kinetic model has been developed for the laser thruster and performance (ISP) of approximately 1500 sec is predicted for the pure hydrogen plasma thruster. Experimental diagnostics have been developed for the determination of plasma temperature and composition by optical means. These diagnostics have been verified for the preliminary test case, a 2.0 atm laser sustained plasma in argon. The spark breakdown threshold has been measured for hydrogen and an experimental technique for pulsed laser plasma ignition has been developed. Further studies which involve the creation of steady-state laser-sustained plasmas in static and flowing hydrogen gas are currently underway.

The principal goal of this program has been the development of an experimental data base for the determination of laser thermal thruster operational feasibility. Although this data base is not yet complete, sufficient interest has been generated to continue the program with the emphasis shifted to the development of a subscale laser thruster for testing. This thruster will be tested in a high altitude simulation facility currently under construction at MSFC.

The development of any flight worthy laser thruster will require not only the successful solution of the plasma absorption problem but also several engineering problems which to date have not been addressed. These problems include an efficient scheme for plasma-fluid thermal mixing for enhanced nozzle performance, regenerative cooling designs for wall protection and advanced film-cooled high power laser windows. These problems will be considered as the program progresses.

APPENDIX

DIAGNOSTICS FOR DETERMINATION OF HYDROGEN LASER-SUSTAINED PLASMA TEMPERATURE

I. Theory of Plasma Radiation

The plasma formed at the focus of a high power laser is, in many respects, the ideal source for atomic spectroscopic analysis. Unlike gaseous arcs, the subject of rigorous study for many years, the laser sustained plasma is spatially well defined and very stable due to the confining nature of the incident beam. The laser beam is axially symmetric in many laser systems; therefore, the use of Abel's inversion is also appropriate for data reduction. No electrodes are necessary, therefore it is possible to study pure gases without the worry of contamination.

The state of a plasma in complete thermodynamic equilibrium is fully specified by the temperature if the total pressures of the component gases are given. The radiation field of such a plasma is that of a black body and may be readily calculated. The laser sustained plasma (LSP) emits copious quantities of optically thin radiation and therefore does not meet the rigorous qualifications of complete thermodynamic equilibrium. However, the LSP is sufficiently dense to satisfy what is known as Local Thermodynamic Equilibrium (LTE). In LTE, the plasma processes are dominated by collisions and the local state of matter is well described by thermodynamic equilibrium. Therefore, the term "temperature" is meaningful in this application and its measurement is quite useful for the purpose of characterizing the plasma state.

A measurement of the optically thin radiation from the plasma allows a non-intrusive (although indirect) determination of the plasma temperature. The total emitted radiation, ε_ν (W/cm Hz sr), at any frequency, ν, for a plasma is given by:

$$\varepsilon_\nu = \varepsilon_\nu^{ff} + \varepsilon_\nu^{fb} + \varepsilon_\nu^{\ell} \quad . \tag{1}$$

In LTE, the radiation of each component above is an explicit function of temperature. Therefore, measurement of any component is sufficient to yield the temperature by reverse interpolation.

If a region of the spectrum away from any spectral lines is chosen for measurement then the line contribution, ε_ν^{ℓ}, is negligible and may be ignored. This assumption greatly simplifies matters as it eliminates the need for tedious line-broadening calculations for interpretation of the results. In practice, the continuum radiation from the plasma at the wavelength of interest may be measured directly using a narrow-band interference filter.

In a region free of lines, the continuum radiation from the plasma is slowly varying and may be considered constant over the narrow bandpass of the filter. Therefore, the spectral radiance of the plasma image at the target wavelength is equal to the radiance of the plasma divided by the effective filter bandwidth. This allows a simple and direct absolute measurement of the continuum component of the plasma emission and hence ready determination of plasma temperature.

The free-free and free-bound continuum radiation for hydrogen is readily calculated using classical theory and quantum mechanical corrections known as Gaunt factors. For the free-bound radiation, Richter [14] gives:

$$\varepsilon_\nu^{fb} = \frac{C_1 N_e N_{Z-1} Z^4}{T_e^{3/2}} \exp\left[\frac{\chi_{z-1} - h\nu}{k T_e}\right] \sum_n G_n(\nu) n^{-3} \exp\left[\frac{-E_n}{k T_e}\right] . \qquad (2)$$

This expression consists of the sum of contributions from all available levels. The series is truncated due to the lowering of the ionization potential produced by the effects of neighboring atoms. The Gaunt factors have been calculated by Karzas and Latter [15] for hydrogenic systems using the quantum defect method.

The free-free continuum radiation is produced when unattached electrons interact. When interacting electrons accelerate or decelerate the energy deficit is balanced by the emission/absorption of continuum radiation. For a plasma with a Maxwellian distribution of electron velocities, Richter gives:

$$\varepsilon_\nu^{ff} = C_2 Z^2 \left[\frac{N_e N_z}{T_e^{1/2}}\right] \exp\left[\frac{-h\nu}{k Te}\right] G^{ff}(\nu) \quad . \qquad (3)$$

The Gaunt factors for the free-free radiation have also been calculated by Karzas and Latter (above) assuming a pure Coulomb potential.

II. Theory of Plasma Composition

The number densities of the various plasma constituents must be calculated for the given conditions before the plasma radiation can be calculated. For a plasma in LTE, the plasma components are related by the Saha equation:

$$\frac{N_e N_z}{N_{z-1}} = 2\left[\frac{U_z(T)\ (2\pi m_o KT)^{3/2}}{U_{z-1}(T)\ h^3}\right] \exp\left[\frac{\chi_{z-1} - \Delta\chi_{z-1}}{KT}\right] \quad . \qquad (4)$$

This equation is an extension of the Boltzmann formula to ionized atoms and only provides information about the relative amounts of each plasma constituent. A complete solution for all plasma parameters requires the addition of two other equations, the equation of state and conservation of charge. The equation of state for a plasma in a Coulombic field is given by:

$$P = kT \sum_i Ni - \frac{kT\ Q^3}{24} \quad . \qquad (5)$$

Here the total pressure is given by P and Ni is the number density of the ith constituent. The extra term in the above formula is the "excess pressure" due to the electrostatic action of the Coulombic field. The quantity, Q, in this term is given by:

$$Q = \frac{e^2}{\varepsilon_o KT} \sum_i Z_i^2 N_i \quad . \tag{6}$$

The overall electrical charge of a plasma is generally zero. This is stated by conservation of charge:

$$\sum_i N_i Z_i = 0 \quad . \tag{7}$$

For a hydrogen plasma, only these three fundamental equations need to be included in order to solve for the three principal species: H, e-, and H+. Note that the diatomic molecule H_2, has been excluded from this analysis. This is because the population of H_2 (and hence, the emission) is orders of magnitude below that of the three species above in the plasma. This disparity in magnitude restricts this diagnostic method to the determination of plasma temperatures above 9000 K only.

A proper solution of this system of equations must also consider the number of energy levels which actually exist for the atom. An isolated atom has an infinite number of possible energy levels for the electron to occupy. When the atom is in the presence of other atoms, its outer levels are perturbed and the actual number of available levels beneath the ionization threshold is finite. The relative probability or "partition" functions for each level are calculated by:

$$U(T) = \sum_n g_i \exp\left[\frac{-Ei}{KT}\right] \quad . \tag{8}$$

here g_i is the "statistical weight" for the ith level. Note that the calculation of the partition function involves a summation over all existing levels, n. The solution of this system of equations would be straight-forward if it were not for the presence of the term $\Delta\chi_{z-1}$ in equation (4) and the need to know the number of existing levels as in equation (8). These two quantities are closely related since the energy of the last level is equal to $\chi_o - \Delta\chi_{z-1}$, which is the reduction of the ionization potential due to the influence of neighboring atoms. This factor is a function of the number densities for which it is required to solve, hence a closed-form solution is not possible. In practice, this equation is rewritten in terms of partial pressures and solved iteratively.

Number density calculations have been performed for hydrogen using the aforementioned methods for pressures ranging from 1 to 3 atm and temperatures from 9000 to 30,000 K. The results for 1 atm are shown in Figure A-1. The lowering of the

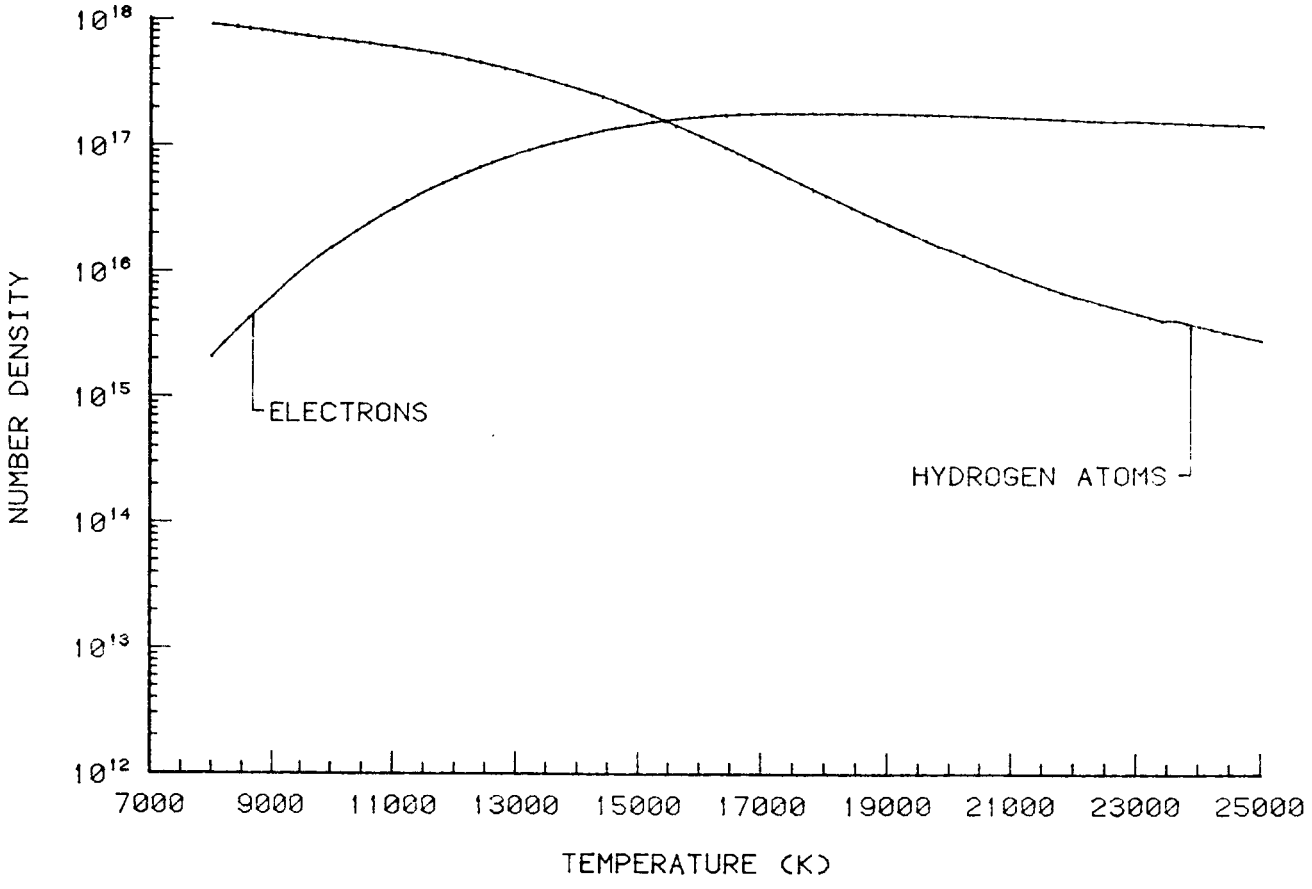

Figure A-1. Calculated number densities for hydrogen at 1.0 atm total pressure.

ionization potential for these calculations was chosen as a parabolic fit between two classical estimates by Unsold [16] and Ecker and Kroll [17]. This fit was chosen to give agreement with the extensive state calculations performed by Patch [18]. This method yielded a simple solution to the Saha equation which closely agrees with the results of Patch for pressures under 5 atm.

III. Calculations of Plasma Radiation

A computer code has been developed to perform the continuum radiation calculations for hydrogen using the techniques as described above. This code, HRAD, will calculate the continuum radiation (both free-free and free-bound) as a function of wavelength for temperatures from 9000 K to 30,000 K at total pressures from 1 to 5 atm. Some results are shown in the figures that follow. In Figure A-2, the total continuum radiation is plotted as a function of wavelength for a temperature of 17,000 K and a pressure of 1 atm. The calculated emission coefficient for hydrogen at a wavelength of 5145 angstroms (corresponding to the wavelength of a popular argon laser-line filter) is plotted as a function of temperature in Figure A-3. The data in Figure A-3 will be useful for the determination of the hydrogen plasma temperature if emission data are taken at that wavelength.

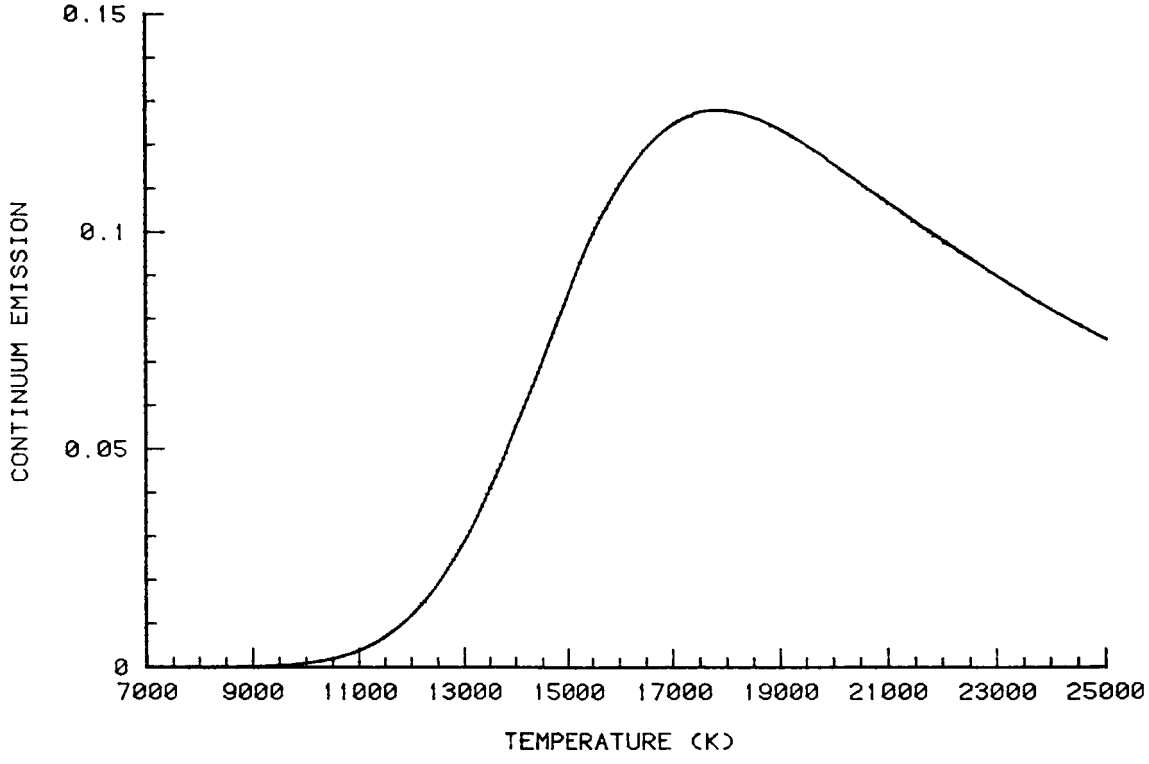

Figure A-2. Calculated total continuum radiation for hydrogen at 1.0 atm and 17,000 K.

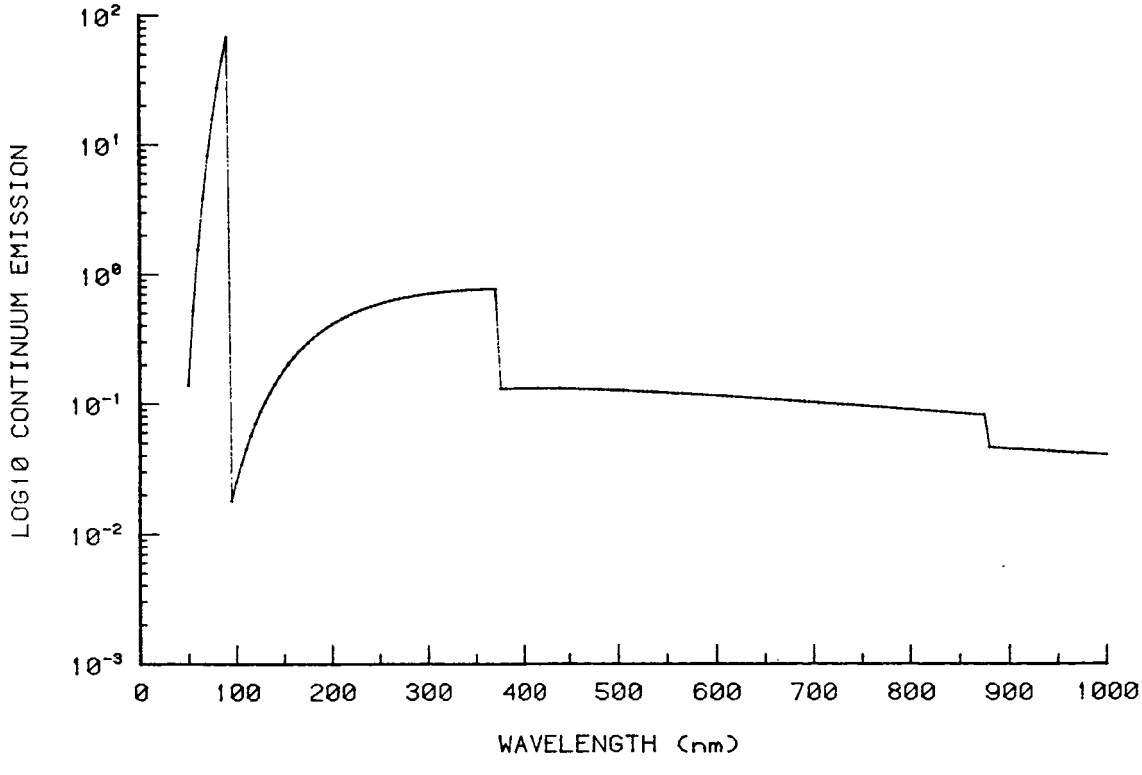

Figure A-3. Calculated emission coefficient for a hydrogen plasma at a wavelength of 5145 A and a pressure of 1.0 atm.

IV. Determination of Plasma Emission

The measurement of radiation from the plasma in the laboratory does not yield the plasma emission coefficient (as calculated above) directly. The emission coefficient ($W/cm^3/sr/Hz$) is a measure of the volumetric radiation from the plasma per unit solid angle per unit frequency interval. In practice, we can only measure the radiance ($W/cm^2/sr$) by direct means. The radiance is a measure of the radiative flux emitted from a surface per unit solid angle and is the natural quantity measured by most detectors.

In order to determine the emission coefficient of a plasma, ε, the three-dimensional spatial distribution of plasma emission must be considered. The radiance profile at a particular point in a plasma image is the result of the integration of all volumetric plasma emission along the line of sight. For the purposes of the proposed analysis, two key assumptions are to be made in the determination of the spatial plasma emission – first, the plasma is assumed to be optically thin, i.e., the emitted plasma radiation is not reabsorbed during its passage through the plasma. Second, the plasma is assumed to be axially symmetric.

The optically-thin axially symmetric radiation source has been studied for many years. The emission coefficient for such sources are generally calculated by inversion of what is known as the "Abel integral." Consider the emission of radiation from a cylindrical source (Fig. A-4). The intensity of radiation falling on the detector due to contributions all along the line of sight is given by:

$$I(x) = 2 \int_x^R \frac{\varepsilon(r)\, r}{[r^2 - x^2]^{1/2}}\, dr \quad . \tag{9}$$

Here I(x) is the measured radiance which is a function of the displacement, x. The radial location is denoted by r and the plasma outer radius is denoted by R.

By substitution using what is known as Abel's transform, equation (9) may be rewritten as:

$$\varepsilon(r) = \frac{1}{\pi} \int_r^R \frac{dI/dx}{[x^2 - r^2]^{1/2}}\, dx \quad . \tag{10}$$

This formulation gives the radial emission coefficient for the given geometry and distribution of plasma radiance. One great difficulty of this method lies in the derivative term, dI/dx. This requires the differentiation of noisy data as input for the emission coefficient solution. The philosophy employed most successfully for the evaluation of this integral has been to curve fit the data, I(x), to least squares polynomials. The integral is then calculated from the resulting polynomial formula explicitly. Shelby [19] has created an Abel inversion code based on this philosophy which also allows tracking of the errors inserted by the inversion process. This code has been successfully modified to allow graphic interaction in choosing the most proper curve fit to the available data and is currently in use for plasma data reduction.

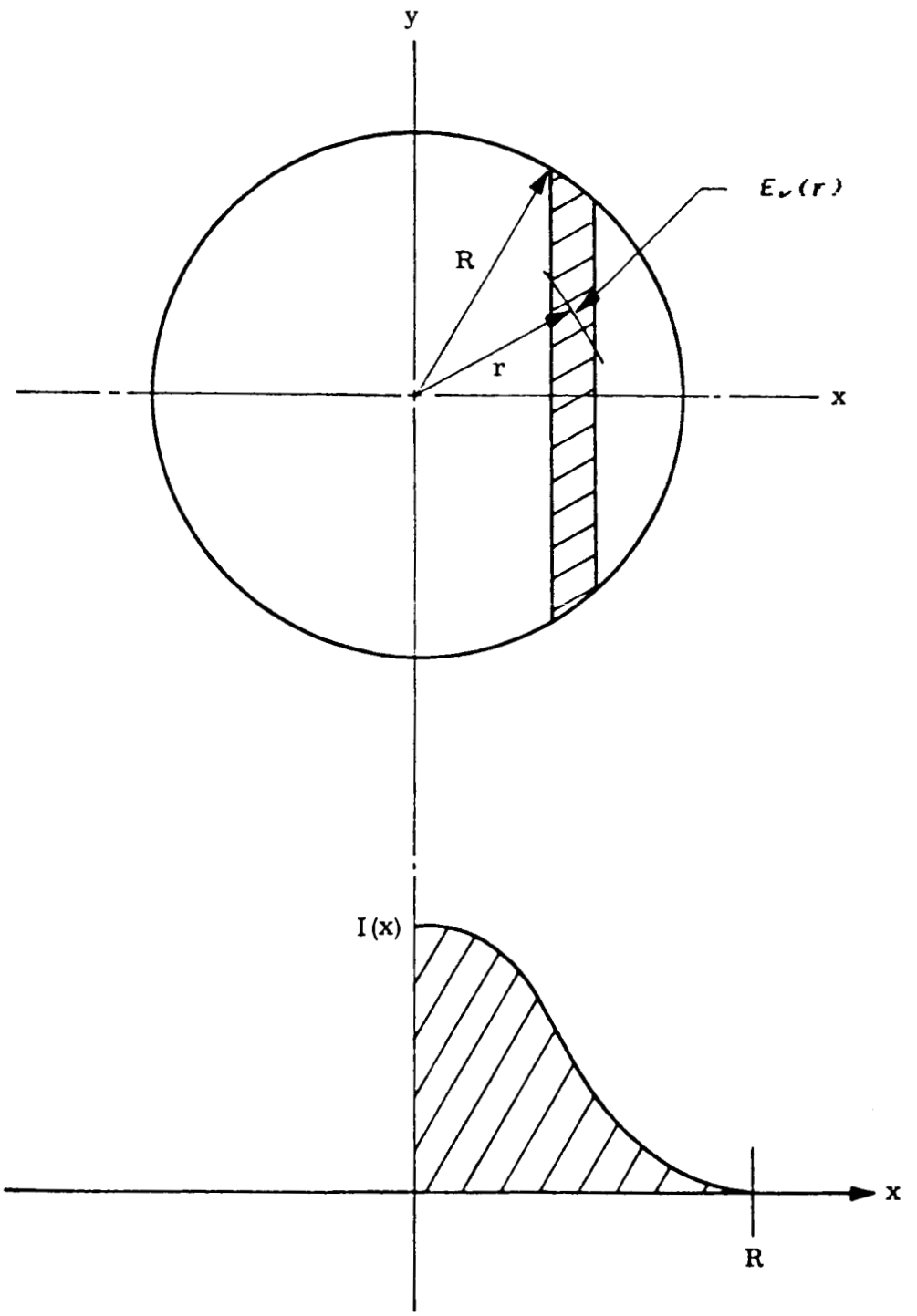

Figure A-4. Geometry of the cylindrical emission source.

The primary plasma diagnostic is based on a measurement of the plasma continuum radiation. This measurement is made using a calibrated CID video camera oriented so that the plasma is "sliced" perpendicular to the plasma axis by each raster scan line (Fig. A-5). The camera is fitted with a narrow-bandpass interference filter in order to provide a monochromatic image of the plasma at the desired wavelength. Camera data is recorded on a commercial grade video recorder for later digitization by a video frame "grabber."

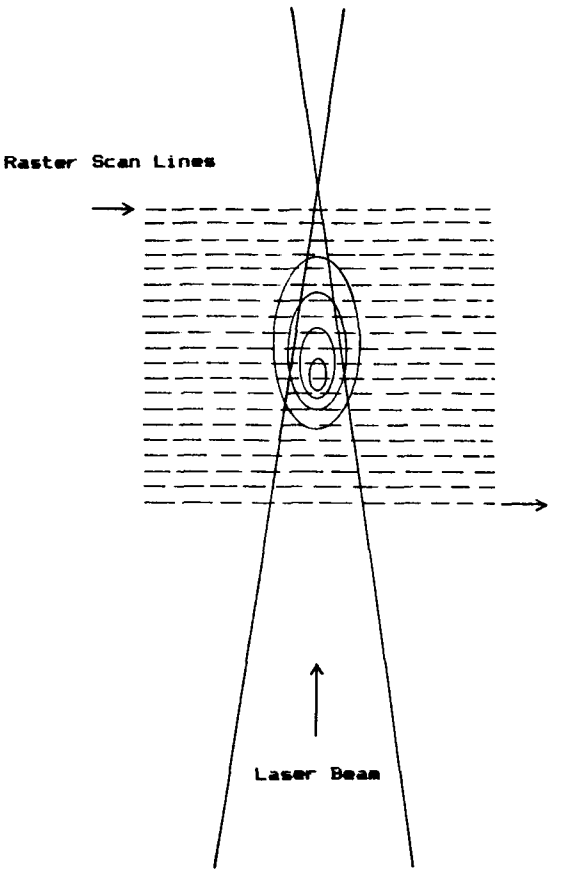

Figure A-5. Raster scan line orientation for plasma data acquisition.

Calibration of the video data acquisition system is accomplished using an NBS traceable standard of spectral radiance. This standard is a specially modified tungsten strip filament lamp fitted with a sapphire window for calibration from the near ultraviolet to the near infrared. The image of the tunsten strip is digitized through the narrow bandpass filter and a varying number of calibrated neutral density filters. In this manner, the camera/recorder/digitizer system response function to varying light intensities at the desired wavelength is determined. The calibration is performed with the standard lamp placed in the exact plasma position in the test chamber. The same camera optics, chamber windows, etc., are used during the calibration to account for any losses and to preserve the original solid angle. In practice, the calibrations are performed immediately following a plasma test in order to eliminate the effects of equipment drift or aging.

Emission spectra of the LSP is taken using an OMA III intensified vidicon spectral measurement system. This system provides nearly simultaneous spectral data to be taken for all points along one spatial dimension of the plasma. This data may be

Abel-inverted to yield either line or continuum measurements of the emission coefficient to allow an additional determination of the plasma temperature by line-line or line-continuum ratio techniques. This spectral data may also be used to check the amount of contamination of the principal continuum diagnostic by the effects of overlapping spectral lines.

V. Application of Method

The above techniques have been used to reduce data from a laser-sustained plasma in 2 atm argon. The emission coefficient of argon was obtained for various pressures and temperatures from a study of arcs by Morris [20]. The experimental data was Abel-inverted to yield emission coefficients which were reduced to temperature by correlation with the given data. A single profile corresponding to the "slice" at the point of maximum temperature is presented in Figure A-6.

The peak temperature of the plasma is exactly that as predicted using the Raizer Hypothesis which states that the peak temperature of the LSP will be the temperature at which the absorption curve peaks. This is because actual power input to the plasma is reduced for higher temperatures due to a decrease in plasma density (and hence absorption coefficient) at constant pressure. For 2 atm argon, this peak occurs at approximately 16,500 K which agrees with the peak of the calculated temperature distribution.

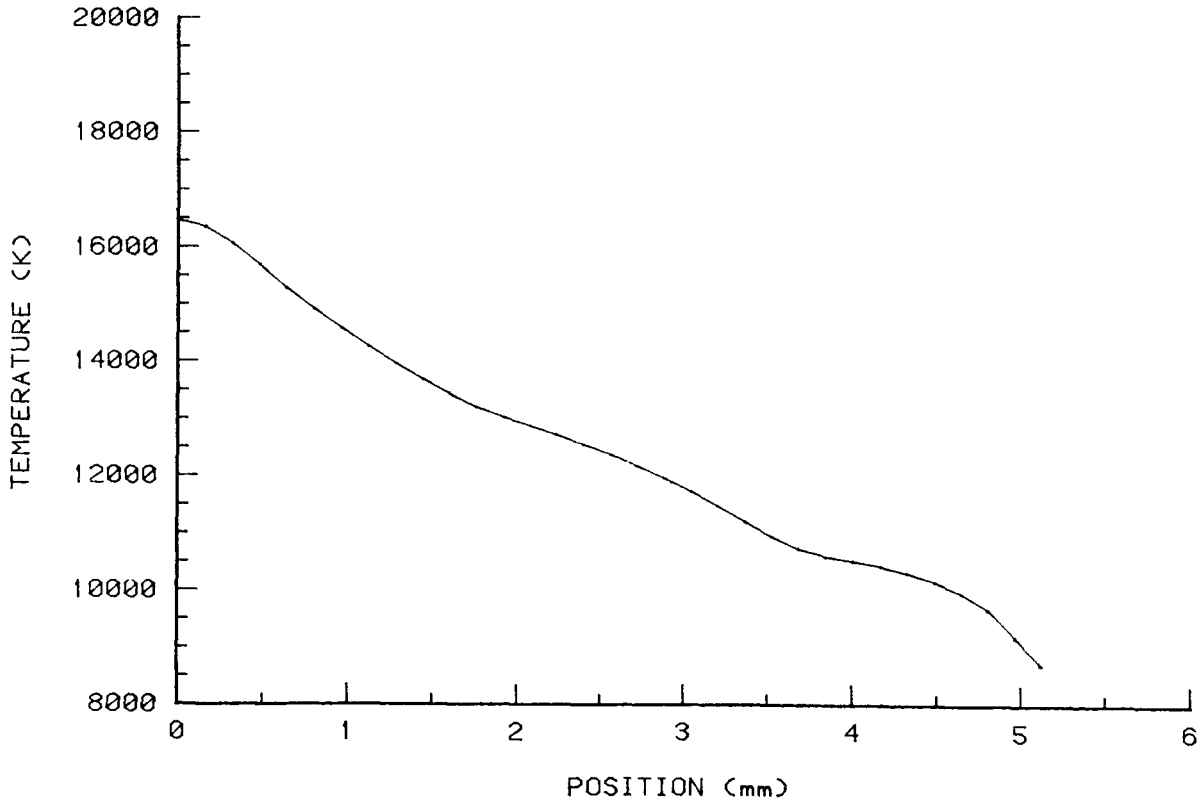

Figure A-6. Temperature profile for a 2.0 atm laser-sustained plasma in argon.

REFERENCES

1. Shoji, J. M.: Laser-Heated Rocket Thruster. NASA CR-135128, May 1977.

2. Bray, K. N.: Atomic Recombination in a Hypersonic Wind Tunnel Nozzle. Journal of Fluid Mechanics, Vol. 6, 1959, pp. 1-32.

3. Nickerson, G. R., et al.: TDK - Two-Dimensional Kinetics Reference Computer Program. Ultrasystems, December 1973.

4. McCay, T. D. and Dexter, C. E.: Chemical Kinetic Performance Losses for a Hydrogen Laser Thermal Thruster. AIAA Paper No. AIAA-85-0907, June 1985.

5. Jones, L. W. and Keefer, D. R.: The NASA Laser Propulsion Project: An Update. AIAA Paper 81-1248, June 1981.

6. Smith, D. C. and Fowler, M. C.: Ignition and Maintenance of a CW Plasma in Atmospheric Pressure Air with CO_2 Laser Radiation. Applied Physics Letters, Vol. 22, No. 10, May 15, 1973.

7. Smith, D. C. and Fowler, M. C.: Ignition and Maintenance of Subsonic Plasma Waves in Atmospheric Pressure by CW CO_2 Laser Radiation and Their Effect on Laser Beam Propagation. Journal of Applied Physics, Vol. 46, No. 1, January 1975.

8. Moody, C. D.: Maintenance of a Gas Breakdown in Argon Using 10.6-m Radiation. Journal of Applied Physics, Vol. 46, No. 6, June 1975.

9. Fowler, M. C., Newman, L. A., and Smith, D. C.: Beamed Energy Coupling Studies. UTRC 203-727-F000, January 1980.

10. Conrad, R. W., et al.: Laser-Supported Combustion Wave Ignition in Hydrogen. U. S. Army Missile Command, Technical Report RH-80-1, October 1979.

11. Keefer, D. R., Henrikson, B. B., and Braerman, W. F.: Experimental Study of an Experimental Laser-Sustained Air Plasma. Journal of Applied Physics, Vol. 46, 1975, p. 1080.

12. Smith, D. C.: Applied Physics Letters, Vol. 19, p. 405.

13. Caressa, J. P., et al.: Breakdown over Long Distances. J. Appl. Physics, Vol. 50, No. 11, November 1979, pp. 6822-6825.

14. Richter, J.: in "Plasma Diagnostics," W. LochteHoltgreven, ed., North Holland Publishing Co., Amsterdam, 1968.

15. Karzas, W. J. and Latter, R.: Astro. Phys. J. Suppl., Vol. 6, No. 55, p. 167, 1961.

16. Unsold, A. Z.: Astrophys., Vol. 24, p. 355, 1948.

17. Ecker, G. and Kroll, W.: Phys. Fluids, Vol. 6, No. 62, 1963.

18. Patch, R. W.: NASA SP-3069, 1971.

19. Shelby, R. T.: Abel Inversion Error Propagation Analysis. Master's Thesis, University of Tennessee, June 1976.

20. Morris, J. C. and Yos, J. M.: Report No. ARL 71-0317.

APPROVAL

AN EXPERIMENTAL STUDY OF LASER-SUPPORTED PLASMA FOR LASER PROPULSION – FINAL REPORT

Center Director's Discretionary Fund Project No. DFP-82-33

By R. H. Eskridge, T. D. McCay, and D. M. Van Zandt

The information in this report has been reviewed for technical content. Review of any information concerning Department of Defense or nuclear energy activities or programs has been made by the MSFC Security Classification Officer. This report, in its entirety, has been determined to be unclassified.

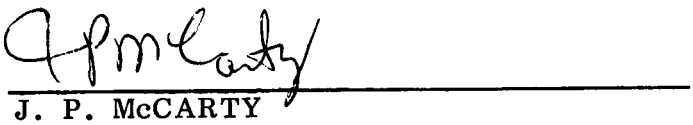

J. P. McCARTY
Director, Propulsion Laboratory

☆U.S. GOVERNMENT PRINTING OFFICE 1987–730-067/40068

TECHNICAL REPORT STANDARD TITLE PAGE

1. REPORT NO.	2. GOVERNMENT ACCESSION NO.	3. RECIPIENT'S CATALOG NO.
NASA TM-86583		

4. TITLE AND SUBTITLE	5. REPORT DATE
An Experimental Study of Laser-Supported Plasmas for Laser Propulsion - Final Report, Center Director's Discretionary Fund Project DFP-82-33	January 1987
	6. PERFORMING ORGANIZATION CODE
7. AUTHOR(S)	8. PERFORMING ORGANIZATION REPORT #
R. H. Eskridge, T. D. McCay, and D. M. Van Zandt	
9. PERFORMING ORGANIZATION NAME AND ADDRESS	10. WORK UNIT NO.
George C. Marshall Space Flight Center Marshall Space Flight Center, Alabama 35812	11. CONTRACT OR GRANT NO.
	13. TYPE OF REPORT & PERIOD COVERED
12. SPONSORING AGENCY NAME AND ADDRESS	Technical Memorandum
National Aeronautics and Space Administration Washington, D.C. 20546	14. SPONSORING AGENCY CODE

15. SUPPLEMENTARY NOTES

Prepared by Propulsion Laboratory, Science and Engineering Directorate.

16. ABSTRACT

The rudiments of a rocket thruster, which receives its enthalpy from an energy source which is remotely beamed from a laser, is described. An experimental study, now partially complete, is discussed which will eventually provide a detailed understanding of the physics for assessing the feasibility of using hydrogen plasmas for accepting and converting this energy to enthalpy. A plasma ignition scheme which uses a pulsed CO_2 laser has been developed and the properties of the ignition spark documented, including breakdown intensities in hydrogen. A complete diagnostic system capable of determining plasma temperature and the plasma absorptivity for subsequent steady-state absorption of a high power CO_2 laser beam are developed and demonstrative use is discussed for the preliminary case study, a two atmosphere laser supported argon plasma.

17. KEY WORDS	18. DISTRIBUTION STATEMENT
CO_2 Lasers, Plasmas, Propulsion, Laser-Heated Thruster, Energy Conversion, Plasma Spectroscopy	Unclassified – Unlimited

19. SECURITY CLASSIF. (of this report)	20. SECURITY CLASSIF. (of this page)	21. NO. OF PAGES	22. PRICE
Unclassified	Unclassified	32	NTIS

MSFC - Form 3292 (May 1969)

For sale by National Technical Information Service, Springfield, Virginia 22151